JOURNAL OF SOLID STATE CHEMISTRY 102, 340–348 (1993)

The Crystal Structure of $Sb_{0.92}V_{0.92}O_4$, Determined by Neutron and Dual Wavelength X-Ray Powder Diffraction

STAFFAN HANSEN* AND KENNY STÅHL

Inorganic Chemistry 2, Chemical Center, University of Lund, P.O. Box 124, S-221 00 Lund, Sweden

AND ROLAND NILSSON AND ARNE ANDERSSON

Chemical Technology, Chemical Center, University of Lund, P.O. Box 124, S-221 00 Lund, Sweden

Received April 6, 1992; in revised form June 15, 1992; accepted June 24, 1992

A phase of approximate composition $SbVO_4$ has been reported in the literature as a key component in new catalysts for the ammoxidation of propane to acrylonitrile. $Sb_{0.92}V_{0.92}O_4$ was prepared by heating equimolar amounts of Sb_2O_3 and V_2O_5 in air at 1073 K for 2 hr. The chemical composition was determined by thermogravimetry and energy dispersive X-ray microanalysis. The crystal structure at 293 K was determined, from three powder diffraction data sets recorded with Cu$K\alpha_1$, Mo$K\alpha$, and 1.040(1)-Å neutron radiation, using the Rietveld method. Crystal data: $Sb_{0.92}V_{0.92}O_4$, $Z = 1$, $a = 4.625(4)$, $c = 3.040(2)$ Å, tetragonal space group $P4_2/mnm$, $M_r = 222.87$, $D_{calc} = 5.69$ g/cm^3. All three data sets yield a cation deficient rutile structure and final profile R-values of 3.5, 6.3, and 3.5%. Bond valence sums, calculated from the experimentally determined bond lengths, indicate the oxidation states to be Sb^{5+} and V^{3+}/V^{4+}, leading to the formula $Sb^{5+}_{0.92}V^{3+}_{0.28}V^{4+}_{0.64}\square_{0.16}O_4$ (the square denotes metal ion vacancies). Bond valence calculations also suggest that $OSb_2\square$ is the most favorable configuration for an oxygen associated with a metal vacancy.

Introduction

Currently there is a great interest in the development of catalysts for use in the industrial conversion of natural gas components to more refined products. One example is the replacement of the older technology for maleic anhydride production using benzene feedstock with modern processes using butane feed (*1*, *2*). Another example concerns the well known SOHIO (BP America) process for the partial oxidation of propylene in the presence of ammonia (ammoxidation) to acrylonitrile (*3*). In this process a multicomponent bismuth molybdate-type of catalyst is used (*4*). During the last decade successful research has been carried out at SOHIO on propane ammoxidation to acrylonitrile, and a process is targeted for commercialization in the near future (*5*, *6*). For the propane process, an antimony vanadium oxide approaching the composition $SbVO_4$ is reported as a crucial catalyst component (*7*). A few catalytic studies related to this new process have appeared in the literature (*8–10*).

* To whom correspondence should be addressed.

0022-4596/93 $5.00

The $SbVO_4$ phase was reported to have the rutile structure (*11*). The authors assumed the valences to be Sb^{3+} and V^{5+}. However, from magnetic measurements (*12*), on a sample prepared in a closed tube, the composition $Sb^{3+}V^{5+}O_4$ could be excluded and the antimony Mössbauer study by Birchhall and Sleight (*13*) showed antimony to be in the oxidation state 5+. These authors reported the formation of a phase with the composition $Sb_{0.92}V_{0.92}O_4$, when heating a 1 : 1 mixture of V_2O_5 and Sb_2O_3 in air at 800°C. When heating the oxides in a sealed gold tube, the product was biphasic and consisted of a phase with the approximate composition $Sb_{0.95}V_{1.05}O_4$, and small amounts of Sb_2O_4 or amorphous antimony oxide, depending on the temperature. Berry *et al.* (*14, 15*) reported similar results. They observed the formation of rutile-type $Sb_{0.91}V_{0.91}O_4$, when heating equimolar amounts of Sb_2O_3 and V_2O_5 in air. Reduced antimony-deficient rutiles and different antimony oxide phases were formed in experiments performed in strictly oxygen-free nitrogen, commercial nitrogen, or closed tube.

In a study of vanadium doped β-Sb_2O_4, Teller *et al.* (*16*) found "$SbVO_4$" to be one of the minor phases in two samples prepared at 850°C. Lattice and positional parameters were refined from powder diffraction data, but no chemical characterization was reported. It was inferred that the deviating structural features of one sample were due to epitaxial growth of "$SbVO_4$" on the crystal faces of β-Sb_2O_4.

From a catalytic point of view, the detailed structure of the oxidized phase is the most urgent issue, since patents report this phase as being superior to one prepared in nitrogen atmosphere (*7*). In this paper we report the structure determination of an oxidized form of rutile-type antimony vanadium oxide using a monophasic sample, prepared by heating a mixture of V_2O_5 and Sb_2O_3 in air. Based on the structural parameters obtained, the possible oxidation states of the metal ions and the type of defect system present in this solid is discussed.

Experimental

Sample preparation. Powders of V_2O_5 (Riedel-de Haën, 99.5%) and Sb_2O_3 (Merck, >99%) in the molar ratio 1 : 1 were mixed by shaking in a flask. The mixture was then ground in an agate mortar and placed in a silica ship in a chamber furnace. A flow of air was passed through the furnace, and the temperature was raised from ambient to 800°C at 10°C/min. The sample was kept at 800°C for 2 hr. After this period, the heating was stopped and the sample was allowed to cool slowly to room temperature in the closed furnace. The sample was investigated as obtained after a light grinding.

Balance experiments. The synthesis of the sample was repeated in a Cahn Thermogravimetric apparatus, system 113, consisting of a Cahn 2000 balance, a furnace, and a temperature controller. The balance and the sample pan were situated in a glass system provided with gas inlet and outlet ports. About 70 mg of a V_2O_5–Sb_2O_3 mixture prepared as described above was put in the sample pan. A flow of dry air was continuously passed through the balance, except at the moment of weighing when the gas flow was temporarily stopped. First, the sample was heated from room temperature to 130°C at 10°C/min and kept there for 30 min in order to remove adsorbed water. The sample was then slowly cooled to room temperature and the weight was recorded. Thereafter the sample was heated to 800°C at 10°C/min, and was kept there for 2 hr before it again was cooled to room temperature and reweighed. A weight increase was observed coupled to the formation of the antimony vanadium oxide phase. Two measurements gave a nominal composition of $SbVO_{4.35\pm0.01}$ or $Sb_{0.92}V_{0.92}O_4$. The precision inherent in the formula $Sb_{0.92}V_{0.92}O_4$ is also compatible

with the stated purity of the reactants Sb_2O_3 and V_2O_5.

X-ray microanalysis. Antimony vanadium oxide powder was mounted on copper stubs with conducting polymer. Energy dispersive X-ray microanalysis was performed at an acceleration voltage of 20 keV in a JSM-840A scanning electron microscope equipped with a Link An10000 analysis system. Most crystal grains were smaller than 1 μm, but some plates reaching 5 μm were also observed and these were analyzed with the beam scanning an area of about 2 × 3 μm. When the oxygen content was calculated, assuming the metal valencies Sb^{5+}/V^{4+} and four oxygen atoms per formula unit, a composition of $Sb_{0.88(2)}V_{0.90(2)}O_4$ was determined by averaging nine analyses.

Cu$K\alpha_1$ powder diffraction. The diffraction pattern was collected with an INEL powder diffractometer equipped with a CPS120 curved position sensitive detector covering 120°, using a flat plate rotating sample holder set for reflection mode. The Cu$K\alpha_1$-radiation was obtained using a primary beam bent quartz monochromator focusing on the detector and a 0.3-mm exit slit. The diffraction data was accumulated for 24 hr. The detector was calibrated from 25 well resolved diffraction peaks from $Pb(NO_3)_2$ collected under equivalent conditions. The $Pb(NO_3)_2$ peak positions were fitted to the calculated 2θ values using a cubic spline function, which was then used by the Rietveld program (*17*).

Mo$K\alpha$ powder diffraction. The diffraction pattern was collected on a Huber single crystal diffractometer equipped with a flat plate spinning sample holder set up in reflection mode, using graphite monochromatized Mo$K\alpha_1\alpha_2$ radiation, a 0.5-mm point focus collimator, and a 0.5-mm detector slit. Data were collected with ω-2θ step scan in the range $11° < 2\theta < 90°$ in steps of 0.02°, each step measured for 100 sec.

Neutron powder diffraction. The sample was packed in a vanadium sample holder of 11 mm diameter and 50 mm height. The diffraction pattern was collected at the powder diffraction beam line at The Neutron Research Laboratory, Studsvik, Sweden, using neutron radiation of wavelength 1.040(1) Å, as calibrated with an Al_2O_3 standard. Data were collected in the range $0.02° < 2\theta < 118.76°$ in steps of 0.08°; each step was measured for approximately 2 min (monitor controlled) with an array of 10 detectors.

The three data sets in the following are referred to as (C), (M), and (N) for Cu, Mo, and neutron diffraction data, respectively.

Refinements

The Rietveld analysis program used for all of the refinements is essentially the LHMP1 program described by Hill and Howard (*18*) modified to fit local input/output formats and to include Chebyshev polynomials for background fitting and a cubic spline calibration function for the CPS120 detector data (*17*). The program minimizes the quantity $\Sigma w_i (Y_{io} - Y_{ic})^2$ with $w_i = 1/Y_{io}$. A pseudo-Voigt function allowing for five-peak asymmetry was used with a Lorentzian component $\gamma = \gamma_1 + \gamma_2 2\theta$, where γ_1, γ_2 and one asymmetry parameter were refined. FWHM was defined as $(U\tan^2\theta + V\tan\theta + W)^{1/2}$, where U, V and W were refined with peaks trunkated at twelve halfwidths. In addition the 2θ-zero point, one preferred orientation, 8 (C), 10 (M) and 5 (N) background (Chebyshev type I) and two unit cell parameters were refined. The structural parameters comprise one scale factor, one positional parameter, x(O), one occupancy factor for Sb/V with a fixed Sb : V ratio of 1.0, and anisotropic temperature factor coefficients for Sb/V and O (M) and (N). Simultaneous refinements of occupancy factor and temperature factors led to unacceptable correlations for (C) and instead the temperature factor coefficients obtained from (M) were used. The refinements

TABLE I

DATA COLLECTION AND REFINEMENT DATA FOR $Sb_{0.92}V_{0.92}O_4$, AT 20°C. SPACE GROUP $P4_2/mnm$, $Z = 1$, $M_r = 222.87$, $D_{calc} = 5.69$ g/cm^3

Radiation	Cu$K\alpha_1$	Mo$K\alpha_{1}\alpha_2$	Neutrons
λ (Å)	1.54060	0.70932 0.71359	1.040(1)
μ (cm^{-1})	1049.1	126.8	0.0867
2θ-range (°)	25–117	11–90	15–115
No. of steps	3012	3950	1251
Max sin θ/λ (Å^{-1})	0.553	0.997	0.811
No. of param. ref.	21	29	24
a (Å)	4.6294(2)	4.6258(2)	4.6217(7)
c (Å)	3.0414(2)	3.0414(2)	3.0378(5)
V (Å^3)	65.180(7)	65.080(7)	64.89(2)
R_p	0.0347	0.0630	0.0349
R_{wp}	0.0483	0.0836	0.0441
GOF	17.63	1.28	1.29
R_F	0.0181	0.0102	0.0042
No. of Bragg reflections	34	169	96

were considered converged when the maximum shift/e.s.d was less than 0.2. Neutron scattering lengths were taken from (*19*), X-ray scattering factors for O^{2-} were taken from (*20*) and scattering factors for Sb^{5+}, V^{3+} as well as anomalous scattering correction factors from (*21*). R-values given are defined as $R_p = \Sigma|Y_{io} - Y_{ic}|/\Sigma Y_{io}$, $R_{wp} = (\Sigma w_i(Y_{io} - Y_{ic})^2/\Sigma w_i Y_{io}^2)^{1/2}$, GOF $= \Sigma w_i(Y_{io} - Y_{ic})^2/(N - P)$ and the derived Bragg R-value, $R_F = \Sigma|F_{ko} - F_{kc}|/\Sigma F_{ko}$. Additional information on data collections and refinements is given in Tables I and II.[1]

[1] See NAPS document No. 04967 for 28 pages of supplementary material. Order from ASIS/NAPS. Microfich Publications, P.O. Box 3513, Grand Central Station, New York, NY 10163. Remit in advance $4.00 for microfiche copy or for photocopy, $7.75 up to 20 pages plus $0.30 for additional pages. All orders must be prepaid. Institutions and organizations may order by purchase order. However, there is a billing and handling charge for this service of $15. Foreign orders add $4.50 for postage and handling, for the first 20 pages, and $1.00 for additional 10 pages of material, $1.50 for postage of any microfiche orders.

The diffraction patterns and their final difference patterns are shown in Fig. 1.

Discussion

In the two X-ray diffraction experiments Sb and V are the dominating scatterers, with some differences in the anomalous scattering terms between the two X-ray wavelengths used. It was nevertheless no problem to identify the oxygen atom as the highest peak in a difference Fourier synthesis including only the metal atoms. In the neutron diffraction experiments on the other hand, Sb and O are the dominant scatterers, while the scattering length of V is almost zero, cf. the sample holder of vanadium metal utilized for the data collection. This difference between X-rays and neutrons is clearly manifested in the relative intensities of the diffraction patterns in Fig. 1.

In view of the experimental differences mentioned above it is encouraging that the structural parameters presented in Tables I and II are in general agreement, especially

TABLE II

REFINED STRUCTURAL PARAMETERS, DISTANCES (Å), AND ANGLES (°) FOR $Sb_{0.92}V_{0.92}O_4$

Data set	(C)	(M)	(N)
x(O)	0.2990(4)	0.3022(5)	0.3028(2)
g(Sb/V) · 16	0.949(6)	0.958(9)	0.917(12)
β_{11}(Sb/V)	0.0061[a]	0.0061(3)	0.0019(10)
β_{33}(Sb/V)	0.0250[a]	0.0250(12)	0.0082(41)
β_{12}(Sb/V)	−0.0019[a]	−0.0019(8)	0.0003(13)
B_{ave} (Å^2)	0.66[a]	0.66(2)	0.21(6)
β_{11}(O)	0.0088[a]	0.0088(16)	0.0072(5)
β_{33}(O)	0.0160[a]	0.0160(51)	0.0241(16)
β_{12}(O)	−0.0086[a]	−0.0086(18)	−0.0010(5)
B_{ave} (Å^2)	0.70[a]	0.70(9)	0.71(3)
Sb/V–O (2×)	1.958(3)	1.977(3)	1.979(1)
Sb/V–O (4×)	2.011(2)	1.997(2)	1.9922(7)
O–Sb/V–O (8×)	90.00	90.00	90.00
O–Sb/V–O (2×)	98.26(13)	99.22(15)	99.36(47)
O–Sb/V–O (2×)	81.74(11)	80.78(13)	80.64(41)
Sb/V–O–Sb/V (2×)	130.87(6)	130.39(7)	130.32(2)
Sb/V–O–Sb/V (1×)	98.26(13)	99.22(15)	99.36(5)

Note. Temperature factor expressions: exp(. . . $-\beta_{ij} \cdot h_i \cdot h_j -$ . . .) and $B_{ave} = 4[\sum_i \sum_j \beta_{ij} \cdot (\mathbf{a}_i \cdot \mathbf{a}_j)]/3$.

[a] Not refined.

the parameters determined using neutron and Mo$K\alpha$ radiation are quite similar. In the case of Cu$K\alpha_1$ data, the spectrum contains only 34 Bragg reflections, and the thermal parameters could not be refined and the distances deviate slightly from those determined with radiation of shorter wavelength. It is evident that the systematic differences between the three experiments are considerably greater than the estimated standard deviations, which is commonly the case due to serial correlation (*22*). Film data obtained in a Guinier–Hägg focusing camera using Cu$K\alpha_1$ radiation and Si as internal standard gave the refined unit cell: $a = 4.6214(3)$, $c = 3.0387(3)$ Å, cf. Table I. The average unit cell determined by four different methods is: $a = 4.625(4)$, $c = 3.040(2)$ Å.

The refinements indicate that $Sb_{0.92}V_{0.92}O_4$ is a cation-deficient rutile-type structure where the metal site contains a random mixture of 46% Sb, 46% V, and 8% vacancies. The three diffraction data sets gave no indication of a lowering of the ideal tetragonal symmetry $P4_2/mnm$, which would allow an ordered cation distribution. Since it is not possible to refine the Sb/V ratio from diffraction data, it was fixed to 1 : 1 in the calculations as determined by X-ray microanalysis. The total occupancy of metal ions could be properly refined and in the neutron case a 92% occupancy was obtained, which was exactly the value determined by thermogravimetry. With X-ray data slightly higher occupancies were obtained.

As can be seen in Table II, the metal site consists of six oxygens in a rather regular octahedron, while the oxygen site consist of three metal atoms forming a planar triangle.

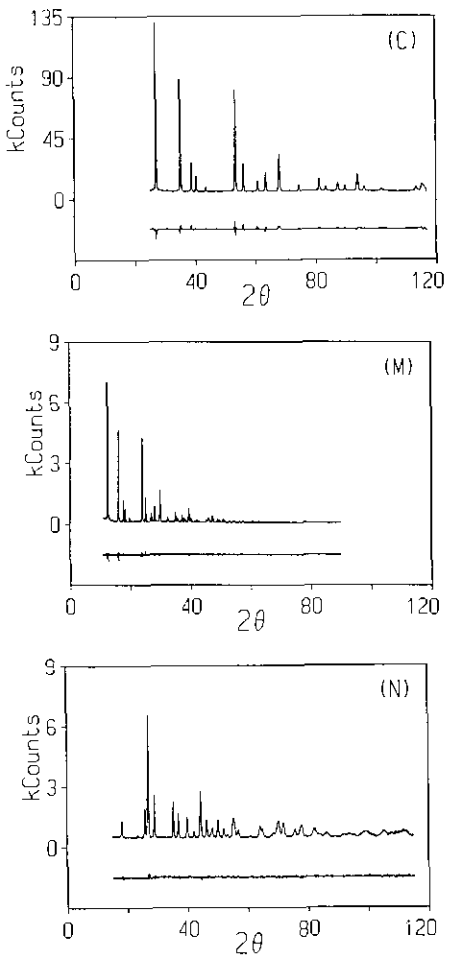

FIG. 1. Diffraction patterns recorded with Cu$K\alpha_1$ (C), Mo$K\alpha_{1}\alpha_2$ (M), and neutron (N) radiation. Final calculated difference patterns are shown below the experimental ones.

$Sb_{0.92}V_{0.92}O_4$ exhibits two shorter bonds and four slightly longer metal–oxygen distances in the octahedron, while rutile proper (TiO_2) exhibits four short bonds (1.948 Å) and two long bonds (1.980 Å); see Ref. (*23*).

In order to test the ability of the oxygen octahedron in $Sb_{0.92}V_{0.92}O_4$ to accommodate Sb and V ions in different oxidation states, bond valence sums of the metal atoms were calculated using bond valences defined as $v = \exp[(R_o - R)/0.37\ \text{Å})]$. Bond-valence parameters (R_o) were taken from Ref. (*24*) and bond lengths (R) determined by neutron diffraction were used; see Table III for results. It is evident that regardless of the R_o used in the calculations, the bond valence sums indicate an atomic valence of 5+ for Sb and between 3+ and 4+ for V.

A similar conclusion will be reached by direct comparison with the average metal–oxygen distances in simple oxides, if the effect of cation coordination number is taken into consideration, cf. corundum-type V_2O_3, 2.01 Å, CN = 6 (*25*); rutile-type VO_2, CN = 6, 1.94 Å (monoclinic, Ref. (*26*)) and 1.93 Å (tetragonal, 360 K, Ref. (*27*)); V_2O_5, CN = 5, 1.83 Å (*28*); senarmontite Sb_2O_3, 1.98 Å, CN = 3 (*29*); and Sb_2O_5, 1.99 Å, CN = 6 (*30*). The observed average distance of 1.99 Å is compatible with the average V–O distances in the V(III) and V(IV) oxides listed, but not that in V(V) oxide, because here the coordination numbers are similar. The two antimony oxides have similar average distances, but the coordination number for the Sb(III) oxide is only half of that for the Sb(V) oxide, which means that six oxygens at a distance of 1.99 Å would lead to an extremely overbonded Sb(III).

It can also be argued that the shape of the oxygen octahedron in itself makes it unsuit-

TABLE III

BOND-VALENCE SUMS OF METAL ATOMS WITH BOND VALENCES CALCULATED AS $v = \exp[(R_o - R)/0.37\ \text{Å})]$ USING BOND-VALENCE PARAMETERS (R_o) FROM REF. (*24*) AND BOND LENGTHS (R) DETERMINED BY NEUTRON DIFFRACTION[a]

R_o/Å	v		Σv
1.973 (Sb^{3+})	0.984 (2×)	0.950 (4×)	5.77
1.942 (Sb^{5+})	0.905 (2×)	0.874 (4×)	5.30
1.743 (V^{3+})	0.528 (2×)	0.510 (4×)	3.10
1.784 (V^{4+})	0.590 (2×)	0.570 (4×)	3.46
1.803 (V^{5+})	0.621 (2×)	0.600 (4×)	3.64

[a] R = 1.979 Å (2×) and 1.992 Å (4×); average 1.988 Å.

able for V^{5+} and Sb^{3+}. V(V) usually exhibits a regular tetrahedral coordination or a distorted square pyramidal coordination with one short V–O distance of about 1.60 Å, as in V_2O_5 (*28*). Sb(III) exhibits a characteristic one-sided three or four coordination; see Ref. (*31*) for a review. By addition of a lone-pair of electrons on the empty side of the coordination sphere, the arrangement can be described as a tetrahedron or a trigonal bipyramid (*32*). Thus, in order to accommodate these two ions considerable local atomic displacements would be required, but the experimental thermal parameters are normal and show no indication of excessive static disorder in the metal or oxygen sites.

Our crystallographic results, which suggest the presence of V(III)/V(IV) and Sb(V) are in good agreement with the results obtained by magnetic measurements (*12*) and Mössbauer spectroscopy (*13*). If all antimony is pentavalent, the average oxidation state of vanadium is 3.70+ and the unit cell content can be formulated as $Sb^{5+}_{0.92}V^{3+}_{0.28}V^{4+}_{0.64}\square_{0.16}O_4$ (the square denotes vacancies), i.e., about $\frac{2}{3}$ of the vanadium is tetravalent.

The bond-valence sum of the oxygen is more complicated to evaluate since the local environment consisting of three metal atoms is variable. Theoretically, the three metal positions can be occupied by a selection of the following: Sb(V), V(III), V(IV), and one vacancy. More than one vacancy per O atom does not seem likely. Nevertheless 16 combinations of species surrounding an oxygen are possible. If the difference between V(III) and V(IV) is neglected, seven combinations still remain.

Bond-valence sums for oxygen, calculated as before, are listed in Table IV. The difference between the calculated valence sum and the expected value for oxygen, i.e., 2, gives an idea of the magnitude and direction of the local distortions of the determined average structure that are needed in order to accommodate an oxygen in a specific crystal environment. Thus for the coordination figure $OSbV_2$ no distortion is required. In the case of $OSb_2\square$, OV_3, and OSb_2V slight distortions are predicted. In the first two cases the oxygen–metal distances will tend to become shorter, while in the last case they will become longer. In the cases of $OSbV\square$, OSb_3, and $OV_2\square$ even larger displacements would be required. There is a big difference in bond-valence sum between the three configurations containing a vacancy, which suggests that $OSb_2\square$ is the most favorable arrangement, followed by $OSbV\square$ and then $OV_2\square$. An oxygen octahedron in a rutile structure is connected to 10 neighboring octahedra by corner- and edge-sharing and it is thus likely that the 10 octahedra surrounding an empty octahedron (a vacancy) will be occupied by more than the five Sb atoms required by stoichiometry.

TABLE IV

BOND-VALENCE SUMS OF OXYGEN CALCULATED[a] FOR DIFFERENT COMBINATIONS OF NEAREST NEIGHBORS

Neighbors	Σv
SbV_2	1.91–2.04
$Sb_2\square$	1.77
V_3	1.55–1.73
Sb_2V	2.28–2.34
$SbV\square$	1.40–1.46
Sb_3	2.65
$V_2\square$	1.03–1.15

[a] R_0 for Sb^{5+}, V^{3+}, V^{4+} and R = 1.988 Å.

In this context it is interesting to note that the structure of Sb_2O_5 (or B–Nb_2O_5) can be described as a rutile structure with a crystallographic shear on (101); see Ref. (*33*). The rutile slabs are two octahedra thick and the slabs are connected by corner-sharing, i.e., via Sb(V)–O–Sb(V) bridges. By varying the thickness of the rutile slabs it is possible, in theory, to change the stoichiometry of the material from MO_2 to MO_3. A phase with

an average slab thickness of six octahedra would have a stoichiometry corresponding to that of the material studied in this paper.

In conclusion, our powder diffraction studies indicate that "$SbVO_4$" prepared in air is a cation-deficient rutile structure with the unit cell content $Sb^{5+}_{0.92}V^{3+}_{0.28}V^{4+}_{0.64}\square_{0.16}O_4$, though further work is needed in order to characterize the crystal defects in this material. The question of whether extended defects are present will be investigated by electron diffraction.

Acknowledgments

Technical assistance by Mr. H. Rundlöf when collecting the neutron powder diffraction data and financial support from the Swedish Natural Science Research Council are gratefully acknowledged. Professor Sten Andersson is thanked for stimulating discussions concerning possible shear mechanisms in rutile structures.

References

1. G. Stefani, F. Budi, C. Fumagalli, and G. D. Suciu, *in* "New Developments in Selective Oxidation" (G. Centi and F. Trifiro, Eds.), Studies in Surface Science and Catalysis, Vol. 55, pp. 537–552, Elsevier, Amsterdam (1990).
2. R. Contractor, J. Ebner, and M. J. Mummey, *in* "New Developments in Selective Oxidation" (G. Centi and F. Trifiro, Eds.), Studies in Surface Science and Catalysis, Vol. 55, pp. 553–562, Elsevier, Amsterdam (1990).
3. R. K. Grasselli and J. D. Burrington, *in* "Advances in Catalysis" (D. D. Eley, H. Pines and P. B. Weisz, Eds.), Vol. 30, pp. 133–163, Academic Press, New York (1981).
4. R. K. Grasselli, J. F. Brazdil, and J. D. Burrington, *in* "Proceedings, 8th Intern. Congr. on Catalysis, Berlin, 1984," Vol. 5, pp. 369–380, Verlag Chemie, Weinheim (1984).
5. Newsletter, *Appl. Catal.* **67,** N5 (1990).
6. J. F. Roth, *in* "Catalytic Science and Technology" (S. Yoshida, N. Takezawa, and T. Ono, Eds.), Vol. 1, pp. 3–13, Kodansha, Tokyo (1991).
7. US Patents 4 746 641 (1988), 4 767 739 (1988), 4 784 979 (1988), 4 788 317 (1988), 4 801 568 (1989), 4 871 706 (1989), 4 879 264 (1989).
8. G. Centi, R. K. Grasselli, E. Patane, and F. Trifiro, *in* "New Developments in Selective Oxidation" (G. Centi and F. Trifiro, Eds.), Studies in Surface Science and Catalysis, Vol. 55, pp. 515–526, Elsevier, Amsterdam (1990).
9. G. Centi, F. Trifiro, and R. K. Grasselli, *Chim. Ind. (Milan)* **72,** 617 (1990).
10. R. Catani, G. Centi, F. Trifiro, and R. K. Grasselli, *Ind. Eng. Chem. Res.* **31,** 107 (1992).
11. L. W. Vernon and W. O. Milligan, *Texas J. Sci.* **3,** 82 (1951).
12. H. Schüer and W. Klemm, *Z. Anorg. Allg. Chem.* **395,** 287 (1973).
13. T. Birchall and A. W. Sleight, *Inorg. Chem.* **15,** 868 (1976).
14. F. J. Berry, M. E. Brett, and W. R. Patterson, *J. Chem. Soc. Dalton Trans.*, 9 (1983).
15. F. J. Berry and M. E. Brett, *Inorg. Chim. Acta* **81,** 133 (1984).
16. R. G. Teller, M. R. Antonio, J. F. Brazdil, and R. K. Grasselli, *J. Solid State Chem.* **64,** 249 (1986).
17. K. Ståhl and R. Thomasson, *J. Appl. Crystallogr.* **25,** 251 (1992).
18. R. J. Hill and C. J. Howard, Australian Atomic Energy Commission (now ANSTO) Report M112, Lucas Heights Research Laboratories, New South Wales, Australia, 1986.
19. L. Koester, H. Rauch, M. Herkens, and K. Schroeder, Kernforschungsanlage Report JUL-1755, Julich, Germany (1981).
20. E. Hovestreydt, *Acta Crystallogr. Sect. A* **39,** 268 (1983).
21. J. A. Ibers and W. C. Hamilton (Eds.), "International Tables for X-ray Crystallography," Vol. IV, Kynoch Press, Birmingham (1974). [present distributor: Kluwer Academic Publishers, Dordrecht]
22. R. J. Hill and I. C. Madsen, *Powder Diffr.* **2,** 146 (1986).
23. S. C. Abrahams and J. L. Bernstein, *J. Chem. Phys.* **55,** 3206 (1971).
24. I. D. Brown and D. Altermatt, *Acta Crystallogr. Sect. B* **41,** 244 (1985).
25. W. R. Robinson, *Acta Crystallogr. Sect. B* **31,** 1153 (1975).
26. J. M. Longo and P. Kierkegaard, *Acta Chem. Scand.* **24,** 420 (1970).
27. D. B. McWhan, M. Marezio, J. P. Remeika, and P. D. Dernier, *Phys. Rev. B* **10,** 490 (1974).
28. H. G. Bachmann, F. R. Ahmed, and W. H. Barnes, *Z. Kristallogr.* **115,** 110 (1961).
29. C. Svensson, *Acta Crystallogr. Sect. B* **31,** 2016 (1975).
30. M. Jansen, *Acta Crystallogr. Sect. B* **35,** 539 (1979).

31. J.-O. BOVIN, "The Hydrolysis of Antimony (III) and the Oxygen Coordination of Antimony (III) in the Solid State," Thesis, Lund (1975).
32. J. GALY, G. MEUNIER, S. ANDERSSON, AND A. ÅSTRÖM, *J. Solid State Chem.* **13,** 142 (1975).
33. S. ANDERSSON AND J. GALY, *J. Solid State Chem.* **1,** 576 (1970).